

CREEP DAMAGE ACCUMULATION AND FRACTURE  
UNDER MULTIAXIAL STRESSES

B.J. Cane

Central Electricity Generating Board,  
Central Electricity Research Laboratories,  
Kelvin Avenue, Leatherhead, Surrey, U.K.

ABSTRACT

The stress state dependence of creep damage accumulation and fracture in coarse grained 2½Cr1Mo and ½CrMoV steels has been studied by conducting tests under uniaxial, biaxial and triaxial stresses. Fracture is shown to result predominantly from the formation and growth of intergranular cavities. These processes are quantified and interpreted mechanistically. Cavity formation is determined by the maximum principal stress,  $\sigma_1$ , while cavity growth depends predominantly on  $\sigma_1$  and the effective stress,  $\bar{\sigma}$ . Accordingly the rupture life is shown, in general, to be a function of both  $\sigma_1$  and  $\bar{\sigma}$ .

KEYWORDS

Creep fracture: intergranular cavitation; cavity nucleation and growth; multiaxial stresses; 2½Cr1Mo steel; ½Cr½Mo½V steel.

INTRODUCTION

Under creep conditions uniaxial data is inadequate in predicting the failure characteristics of material subjected to a multiaxial stress state. This is due to the fact that creep deformation and creep rupture can be dependent upon different multiaxial stress criteria which cannot be differentiated by uniaxial testing (Johnson, Henderson and Khan, 1962). As a consequence, depending on the stress state associated with a particular component geometry, design and integrity assessment methods can be in error if based only on uniaxial rupture data or uniaxial strain limits.

SIGNIFICANT STRESS COMPONENTS

Following the laws for prediction of the onset of plasticity under multiaxial stresses it has generally been found that when shear processes predominate the deformation rate under creep conditions is dictated by the effective stress,  $\bar{\sigma}$ , otherwise known as the second stress invariant or Von Mises equivalent stress, i.e.,

$$\bar{\sigma} = \frac{3}{\sqrt{2}} \tau_{\text{oct}} = \frac{1}{\sqrt{2}} \left[ (\sigma_1 - \sigma_2)^2 + (\sigma_2 - \sigma_3)^2 + (\sigma_3 - \sigma_1)^2 \right]^{1/2} \quad (1)$$

where  $\tau_{\text{oct}}$  is the octahedral shear stress and  $\sigma_1, \sigma_2, \sigma_3$  are the principal stresses.

The stress criterion relevant to creep rupture under multiaxial stresses is by no means as readily determined. It is dependent on the processes leading to creep fracture which may generally be summarised by the following stages:

- I The production of cavity nuclei
- II The formation of stable cavities and their growth to produce discrete cracks, e.g. single grain facet (sgf) cracks in the case of intergranular cavitation.
- III Linkage of discrete cracks and final fracture propagation.

These stages are briefly considered below.

In the absence of pre-existing cavity nuclei (e.g. non-wetting particles) the production of a cavity nucleus requires an accumulation of shear strain. For Stage I the time,  $t_I$ , required to produce a cavity nucleus will thus be dependent only upon  $\bar{\sigma}$ . (N.B. If non-wetting particles are present then  $t_I = 0$ ).

In Stage II the formation of stable cavities is dictated either by the principal stress, e.g. maximum principal stress,  $\sigma_1$ , or by the hydrostatic stress,  $\sigma_H = (\sigma_1 + \sigma_2 + \sigma_3)/3$ . At low strain rates cavity stability can occur at grain boundaries as a result of vacancy supersaturation promoted by  $\sigma_1$ ; a stable cavity forms when the nucleus radius,  $r > 2\gamma/\sigma_1$  where  $\gamma$  is the surface energy (Baluffi and Siegle, 1957). At high strain rates and lower temperatures plastic void formation processes predominate and the cavity stability criterion becomes  $r > 2\gamma/\sigma_H$ . The growth of cavities has been the subject of considerable debate for many years. Only recently has quantitative evidence been obtained to help resolve the situation (Dyson and Loveday, 1980; Cane, 1980; Needham and Gladman, 1980). At low strain rates the basic mechanism of cavity growth is likely to be one of vacancy diffusion although the rate limiting process is sensitive to material and test conditions. If growth is diffusion controlled then it is dictated by the normal grain boundary stress so that  $\sigma_1$  is the significant multiaxial stress component (Speight and Beere, 1975). At higher strain rates the rigid grain assumption implicit in diffusion controlled growth models no longer pertains and the normal stress profile between adjacent cavities can be relaxed by shear deformation, (Beere and Speight, 1978). Accordingly, cavity growth is independent of cavity spacing and becomes increasingly dependent upon  $\bar{\sigma}$  as the strain rate increases such that at high strain rates a plastic or continuum growth process is anticipated. The significant stress components then become  $\bar{\sigma}$  and  $\sigma_H/\bar{\sigma}$ . (Hellan, 1975). If, on the other hand, cavitation occurs in a spatially non-uniform manner (as is normally the case in engineering materials) then under certain conditions cavity growth can become geometrically constrained such that it is controlled by the creep rate (Dyson, 1976). Under these circumstances growth will be dependent on  $\bar{\sigma}$  and the deviatoric stress. Accounting for cavity formation and growth, therefore, the time,  $t_{II}$ , required to achieve a discrete or sgf crack from first nucleation will generally be dependent on  $\sigma_1, \sigma_H$  and  $\bar{\sigma}$ .

The processes involved in Stage III of fracture will again be sensitive to material and test conditions. In a rigid grain situation as might be obtained at low strain rates or in the case of high strength grains a diffusion controlled crack linkage process dependent only upon the maximum principal stress,  $\sigma_1$ , is conceivable (Vitek, 1978). With increasing strain rate, in a similar manner to cavity growth, normal stresses can be relaxed and  $\bar{\sigma}$  becomes increasingly significant. At

high strain rates a crack growth mechanism analogous to continuum hole growth is envisaged and so will depend on  $\bar{\sigma}$  and  $\sigma_H/\bar{\sigma}$ . (Hellan, 1975). Final failure propagation can occur in a range of modes between two extremes: ductile or brittle. Ductile fracture occurs as a result of the above continuum growth process. Brittle fracture involves the propagation of a crack of critical size through the damaged structure in a direction normal to  $\sigma_1$ . Under these circumstances we can advocate a fracture mechanics approach to creep failure such that the critical crack size will be determined by  $\sigma_1$ . The time,  $t_{III}$ , required for linkage of discrete cracks to give final failure propagation will thus, in general, again be a function of  $\sigma_1, \sigma_H$  and  $\bar{\sigma}$ .

The three stages of creep fracture described above will, in many cases, occur simultaneously. Nevertheless, we can identify the stress state dependence of rupture life, in terms of the summation  $t_I + t_{II} + t_{III}$ . For given conditions of stress and temperature the relative significance of each stage of fracture will be sensitive to material factors such as grain size and susceptibility to cavitation. This paper reports on the stress state functions specific to creep damage assessment and failure prediction in  $2\frac{1}{2}\text{Cr}1\text{Mo}$  and  $\frac{1}{2}\text{Cr}\frac{1}{2}\text{Mo}\frac{1}{2}\text{V}$  steels.

#### EXPERIMENTAL

Commercial casts of  $2\frac{1}{2}\text{Cr}1\text{Mo}$  and  $\frac{1}{2}\text{Cr}\frac{1}{2}\text{Mo}\frac{1}{2}\text{V}$  steels were heat treated to yield tempered, coarse grained bainitic structures (grain size  $\approx 150\mu\text{m}$ ). Creep testing was conducted at  $565^\circ\text{C}$  under uniaxial, biaxial and, triaxial conditions. Biaxial tests were performed by direct double shear (Henderson and Sneddon 1972) on cylindrical specimens (diam.=6mm) and torsion tests on thin walled tubular specimens (outer diam.=9mm; wall thickness = 1.3mm). In each case the stress state may be defined,  $\sigma_1/\bar{\sigma} = 1/\sqrt{3}$ . A triaxial stress state was achieved using circumferentially grooved circular notch specimens (bar radius/notch throat radius = 1.9; notch radius/notch throat radius = 0.5). This geometry enabled a reasonably constant stationary state value of  $\sigma_1/\bar{\sigma} (\approx 2)$  to be achieved at the centre of the notch throat. (Hayhurst, Leckie and Henderson, 1977). For each stress state an assessment of cavitation damage on failed and interrupted test specimens was obtained by a quantitative method involving scanning electron fractography (Cane and Greenwood, 1975).

#### RESULTS

Over the major range of effective stresses ( $\bar{\sigma}$ ) examined the mode of failure was predominantly 'brittle' intergranular for all stress states. In uniaxial tension, ( $\sigma_1/\bar{\sigma} = 1$ ) however, at high  $\bar{\sigma}$ , ( $>200\text{MPa}$ ) the rupture mode became 'ductile' transgranular in  $2\frac{1}{2}\text{Cr}1\text{Mo}$  steel. Yet for the same  $\bar{\sigma}$ , the rupture mode remained intergranular for the stress state,  $\sigma_1/\bar{\sigma} = 1.9$  obtained in notch tests.

For a given  $\bar{\sigma}$  an intergranular fracture mode is thus favoured by high  $\sigma_1$  values. The effect is markedly reflected in the rupture life at all  $\bar{\sigma}$  levels. (Fig. 1). Fig. 1(a) shows effective strain - time curves obtained for uniaxial tension and torsion ( $\sigma_1/\bar{\sigma} = 1/\sqrt{3}$ ) in  $2\frac{1}{2}\text{Cr}1\text{Mo}$  and  $\frac{1}{2}\text{Cr}\frac{1}{2}\text{Mo}\frac{1}{2}\text{V}$  steels. Whilst for a given  $\bar{\sigma}$  value, the creep responses in the early stages are similar for tension and torsion, the rupture lives and rupture ductilities are considerably greater in torsion than in tension. Similar results have been obtained in Nimonic 80A (Dyson and McLean, 1977). Torsion test results together with those obtained in double shear and notch tests are included in Fig. 1(b) where the rupture life,  $t_R$ , is shown as a function of  $\sigma_1$  for constant values of  $\bar{\sigma}$ . In general  $t_R$  is dependent upon both  $\sigma_1$  and  $\bar{\sigma}$  although with decreasing  $\bar{\sigma}$  the results for  $2\frac{1}{2}\text{Cr}1\text{Mo}$  steel indicate that  $t_R$  becomes progressively less sensitive to  $\bar{\sigma}$ . Where intergranular cavitation predominates as the damage mode we can thus express the rupture life:

$$t_R \propto 1/\sigma_1^p \bar{\sigma}^{m-p} \quad (2)$$

where  $m$  is the slope of the log stress ( $\sigma$ ) - log rupture life curve for uniaxial tension, i.e.  $m = -\partial \ln t_R / \partial \ln \sigma$  and  $p$  is the slope of the iso- $\bar{\sigma}$  plots in Fig. 1(b), i.e.  $p = -\partial \ln t_R / \partial \ln \sigma_1$ . In the intergranular failure regime, for 2½Cr1Mo steel ( $\bar{\sigma} < 200$ MPa)  $p \approx 2.5$  and  $m$  varies from 12 at high  $\bar{\sigma}$  (>150MPa) to around 3.5 for  $\bar{\sigma} < 80$ MPa. For ½CrMoV steel at  $\bar{\sigma} = 250$ MPa,  $p \approx 3$  and  $m \approx 13$ . In 2½Cr1Mo steel at higher strain rates (i.e.  $\dot{\sigma} > 200$ MPa) results for tension and double shear indicate a smaller value of  $p$  ( $\approx 1.5$ ) perhaps reflecting the change in failure mode to ductile transgranular under such conditions.

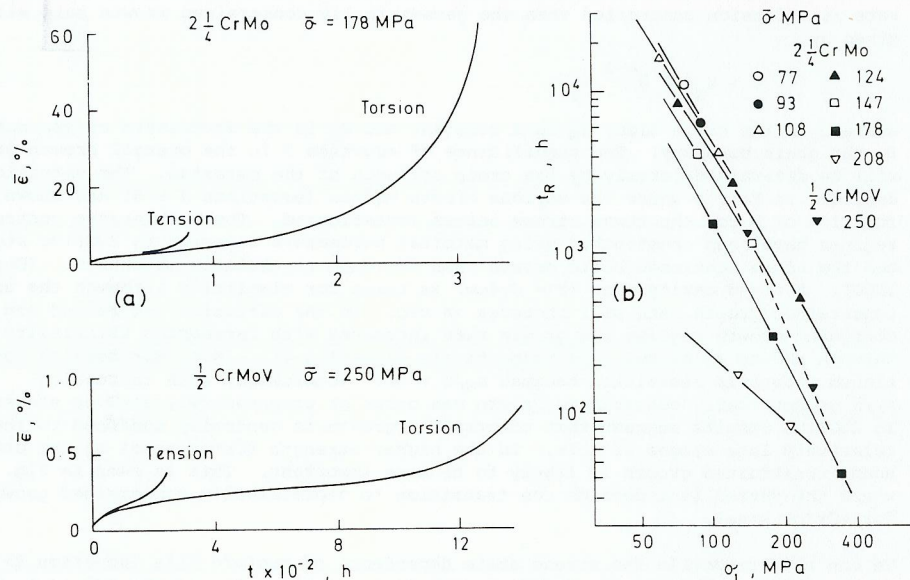


Fig. 1 (a) Effective strain ( $\bar{\epsilon}$ ) - time curves under tension and torsion. (b) Variation in rupture life,  $t_R$ , with  $\sigma_1$  for various  $\bar{\sigma}$ .

By quantitative metallographic methods the above stress state dependence of rupture has been investigated in terms of the cavitation damage processes leading to rupture. Cavities were heterogeneously distributed throughout the prior austenite grain boundaries and were often observed in association with sulphide particles (Cane and Middleton, 1980). In 2½Cr1Mo the number of resolvable cavities per unit grain boundary area,  $N$ , (resolution limit  $\approx 0.2 \mu\text{m}$ ) is plotted as a function of time for the three stress states examined at various  $\bar{\sigma}$  in Fig. 2(a).

Cavities form predominantly during the early stages and the observed rate of formation falls thereafter. For a given time and similar  $\bar{\sigma}$  values the cavity population increases as  $\sigma_1/\bar{\sigma}$  is increased from the torsion situation to uniaxial tension to the notch test situation. In Fig. 2(b) the number of cavities measured during the

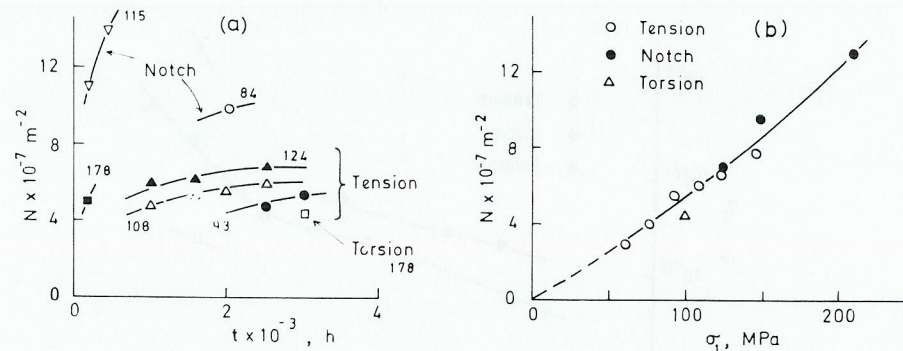


Fig. 2. (a) Variation in number of cavities,  $N$ , with time for notch, tension and torsion tests in 2½Cr1Mo steel.  $\bar{\sigma}$  values are given in MPa.

(b)  $\sigma_1$  dependence of  $N_{\text{max}}$

late stages of creep ( $N_{\text{max}}$ ) is plotted as a function of  $\sigma_1$  for various  $\bar{\sigma}$  in the intergranular failure regime. A good correlation is found with  $\sigma_1$  for torsion, tension and notch tests. Results may be represented by the form:

$$N_{\text{max}} \approx k_N \sigma_1^v \quad (3)$$

where  $v \approx 1.3$  and  $k_N$  is a constant. The value of  $\bar{\sigma}$  is not found to be significant in determining the number of cavities formed.

For all stress states examined the cavity growth rate was found to be directional with respect to the grain boundaries. The largest cavities invariably resided on grain boundaries orientated normal to the maximum principal stress,  $\sigma_1$ . Growth occurred in an approximately spherical manner for cavity sizes up to about  $1 \mu\text{m}$  diameter, thereafter it occurred preferentially in the grain boundary plane. The cavity size in 2½Cr1Mo steel was measured in terms of mean volume  $\bar{v}$  at various times prior to failure. By averaging over these times a mean rate of increase in  $\bar{v}$  was obtained, i.e.  $\dot{\bar{v}}$ . The latter is plotted against  $\bar{\sigma}$  for tension, notch and torsion test conditions in Fig. 3.

For given  $\bar{\sigma}$  values the cavity growth rate increases as the stress state is changed from torsion to notch test situations. A dependence of cavity growth on  $\sigma_1$  is thus evident thereby implying that diffusion controlled growth is significant. However in uniaxial tension the stress sensitivity of cavity growth increases at high  $\bar{\sigma}$  in a manner similar to that of the creep rate. This suggests that the creep strain rate is important in determining the growth kinetics at high  $\bar{\sigma}$ .

In both 2½Cr1Mo and ½CrMoV steels cavity linkage and the formation of sgf cracks occurs in the late stages of life. This results largely from the relatively coarse grain size in each material. The time required for linkage of sgf cracks to give final fracture propagation is thus relatively small.

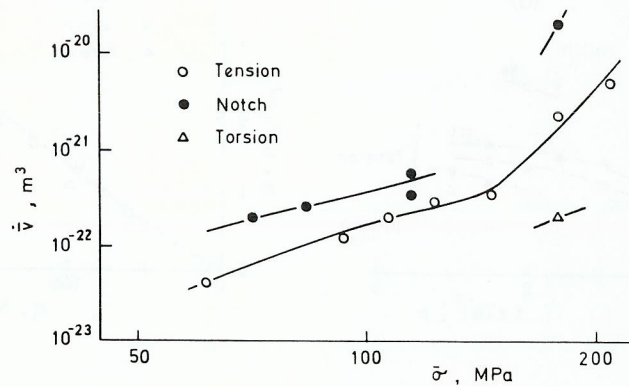


Fig. 3. Variation in mean cavity growth rate,  $\dot{v}$ , with  $\bar{\sigma}$  for notch, tension and torsion tests in  $2\frac{1}{4}\text{Cr1Mo}$  steel

#### DISCUSSION

The above results indicate that Stage II of the creep fracture process is dominant in both coarse grained  $2\frac{1}{4}\text{Cr1Mo}$  and  $\frac{1}{2}\text{CrMoV}$  steels, i.e.  $t_{II} \gg t_I, t_{III}$ . The multi-axial stress rupture criterion will thus be determined largely by the stress state dependences of cavity formation and growth kinetics. These processes are interpreted mechanistically below.

The dependence of cavity population on  $\sigma_1$  and insensitively to  $\bar{\sigma}$  (Fig. 2) implies that decohesion required to produce cavity nuclei and growth of nuclei to a critical size are relatively unimportant events. It can be considered that cavities are produced predominantly from stable nuclei which are instantaneously formed on application of a normal grain boundary stress, (i.e.  $t_I = 0$ ). The observed association of cavities with sulphide particles suggests therefore that the latter behave as relatively incoherent particles. The cavity formation process thus appears to be consistent with classical nucleation theory in which stable cavities form at pre-existing nuclei having radii greater than  $r(=2\gamma/\sigma_1)$ . On this basis the  $\sigma_1$  dependence of the cavity population in Fig. 2(b) can be rationalized in terms of a model in which the size distribution of cavity nuclei may be related to the size distribution of incoherent particles residing in the grain boundaries, (Cane and Middleton, 1980). The expression in equation 2 consequently represents a general form in which the exponent,  $\nu$ , will be determined by the form of the cumulative size distribution curve. (NB. the time dependence of  $N$  in Fig. 2(a) is explicable in terms of a finite time required for growth of cavities to a resolvable size).

The stress and stress state dependence of the cavity growth rate (Fig. 3) may be interpreted in terms of a combined diffusion-deformation controlled growth model (Beere and Speight, 1978). Thus, as discussed earlier, diffusion controlled growth predominates at low strain rates. Accordingly the growth rate will depend

only on  $\sigma_1$  since in the present case the cavity spacing  $c(\propto 1/\sqrt{N})$  is solely a function of  $\sigma_1$  (equation 3). With increasing  $\bar{\sigma}$  the creep rate,  $\dot{\epsilon}(\propto \bar{\sigma}^n)$  becomes increasingly significant and continuum growth (dependent on  $\bar{\sigma}$  and  $\sigma_H$ ) occurs at high strain rates. The cavity growth rate is obtained by summing the two processes, i.e.:

$$\dot{v} \sim K_D A(c, r) [\sigma_1 - \sigma_G] + K_C B(c, r) \bar{\sigma}^n f(\sigma_H/\bar{\sigma}) \quad (4)$$

where  $A$  and  $B$  are functions of cavity size ( $r$ ) and spacing ( $c$ ),  $K_D$ ,  $K_C$  are constants and  $\sigma_G$  is a threshold stress for cavity growth brought about by the surface energy term ( $2\gamma/r$ ) and by the presence of grain boundary carbide precipitates (Harris, 1973; Cane, 1980). Owing to the spatial non-uniformity of cavitation in the present materials growth can become geometrically constrained if the strain rate due to unconstrained cavity growth exceeds the creep rate. If the unconstrained growth rate is diffusion controlled then the geometrically constrained growth rate will be given by

$$\dot{v} \sim K_G d c^2 \bar{\sigma}^{n-1} S_1 \quad (5)$$

where  $d$  is the grain size,  $K_G$  is a constant and  $S_1$  is the deviatoric stress normal to the grain boundary. The significance of equation 5 in the overall growth process will be determined largely by the creep strength of the material. The situation is depicted in Fig. 4 where the various growth models (equations 4 & 5) are shown as a function of  $\bar{\sigma}$  for the three stress states investigated. The mechanistic control regimes have been constructed using material parameters relevant to  $2\frac{1}{4}\text{Cr1Mo}$  steel and the afore mentioned basic growth laws for each controlling mechanism. (Cane, 1980). A fixed cavity size ( $r = 0.4\mu\text{m}$ ) is taken for simplicity although the unconstrained growth rate will increase as  $r \rightarrow c$ . In the diffusion controlled and continuum growth regimes the growth rate increases with increasing triaxiality through the terms  $\sigma_1$  and  $\sigma_H/\bar{\sigma}$  respectively (equation 4). (N.B. For torsion continuum growth is restricted because  $\sigma_H/\bar{\sigma} = 0$ ). Accordingly with increasing  $\sigma_1/\bar{\sigma}$  geometrically constrained growth can occur at progressively earlier stages. In  $2\frac{1}{4}\text{Cr1Mo}$  results suggest that constrained growth is generally confined to the relatively late stages of life. In the higher strength  $\frac{1}{2}\text{CrMoV}$  steel on the other hand, constrained growth is likely to be more important. This is seen in Fig. 4 where the dotted line denotes the transition to geometrically constrained growth for  $\frac{1}{2}\text{CrMoV}$  steel.

We can thus reconcile the stress state dependence of rupture life (equation 2) in terms of the  $\sigma_1$  dependence of cavity formation (equation 3) and the relative significance of the growth processes in equations 4 and 5. At low strain rates in  $2\frac{1}{4}\text{Cr1Mo}$  steel diffusion controlled growth occurs and the first term in equation 4 is dominant; rupture is correspondingly dependent mainly on  $\sigma_1$ . At high strain rates the second term in equation 4 predominates for both  $2\frac{1}{4}\text{Cr1Mo}$  and  $\frac{1}{2}\text{CrMoV}$  steels. Under these circumstances the associated high creep exponent,  $n$ , means that rupture is mainly dependent upon  $\bar{\sigma}$ . Growth governed by equation 5 is likely to be significant at low stresses in  $\frac{1}{2}\text{CrMoV}$  steel such that rupture will again be determined largely by  $\bar{\sigma}$  particularly at high  $\sigma_1/\bar{\sigma}$  values as obtained in the notch tests.

#### CONCLUSIONS

Studies of creep damage accumulation and fracture in coarse grained  $2\frac{1}{4}\text{Cr1Mo}$  and  $\frac{1}{2}\text{CrMoV}$  steels under various stress states at  $565^\circ\text{C}$  have revealed the following points:

1. The multi-axial stress rupture criterion is determined predominantly by the stress state dependences of intergranular cavity formation and growth. The initial production of cavity nuclei and final crack linkage are relatively unimportant stages.

- For a given effective stress,  $\bar{\sigma}$ , brittle intergranular fracture is promoted by increasing  $\sigma_1/\bar{\sigma}$  where  $\sigma_1$  is the maximum principal stress.
- Quantitative metallography indicates that the number of cavities formed is a function of  $\sigma_1$ . The cavity growth rate, in general depends mainly on  $\sigma_1$  and  $\bar{\sigma}$ . The controlling growth mechanism and hence its stress state dependence varies with  $\bar{\sigma}$  and  $\sigma_1/\bar{\sigma}$ . At low  $\bar{\sigma}$  growth in 2½Cr1Mo steel depends predominantly on  $\sigma_1$  while  $\bar{\sigma}$  dominates at high  $\bar{\sigma}$ . At high  $\sigma_1/\bar{\sigma}$  as obtained in notch tests growth can become limited by the creep rate and hence dependent upon  $\bar{\sigma}$ .
- In general the rupture life will be a function of both  $\sigma_1$  and  $\bar{\sigma}$  with  $\sigma_1$  predominating at low  $\bar{\sigma}$  values in 2½Cr1Mo steel. Consequently integrity assessment methods based on uniaxial rupture data or strain limits will be pessimistic in components where  $\sigma_1/\bar{\sigma} < 1$  and optimistic where  $\sigma_1/\bar{\sigma} > 1$ .

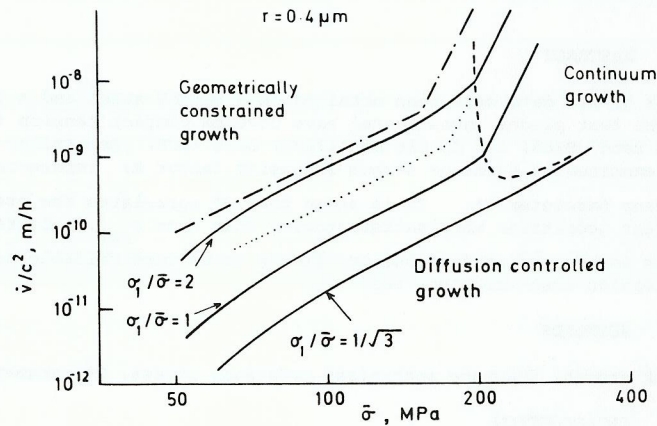


Fig. 4. Effect of  $\bar{\sigma}$  on controlling cavity growth models in 2½Cr1Mo steel for stress states obtained in torsion ( $\sigma_1/\bar{\sigma} = 1/\sqrt{3}$ ), in tension ( $\sigma_1/\bar{\sigma} = 1$ ) and in notch tests ( $\sigma_1/\bar{\sigma} = 2$ )

#### ACKNOWLEDGEMENT

This paper is published with the permission of the Central Electricity Generating Board.

#### REFERENCES

- Baluffi, R.W. and L.L. Siegle (1957) *Acta Met.*, 5, 449.  
 Beere, W. and M.V. Speight (1978). *Metal Science*, 12, 172.  
 Cane, B.J. and G.W. Greenwood (1975) *Metal Science*, 9, 55.  
 Cane, B.J. (1980) to be published.  
 Cane, B.J. and C.J. Middleton (1980) to be published.  
 Dyson, B.F. (1976). *Metal Science*, 10, 349.  
 Dyson, B.F. and D. Mclean (1977) *Metal Science*, 11, 37.

- Dyson, B.F. and M. Loveday (1980) to be published.  
 Hayhurst, D.R., F.R. Leckie and J.T. Henderson (1977) *Int. J. Mech. Science*, 19, 147.  
 Hellan, K. (1975) *Int. J. Mech. Science*, 17, 369.  
 Henderson, J. and J.D. Sneddon (1972) *J. Inst. Metals*, 100, 163.  
 Needham, N.G. and T. Gladman (1980) *Metal Science*, 14, 64.  
 Speight, M.V. and W. Beere (1975) *Metal Science*, 9, 190.  
 Vitek, V. (1978) *Acta Metallurgica*, 26, 1345.